JOURNAL OF CHEMICAL & ENGINEERING DATA

Article

pubs.acs.org/jced

Density, Viscosity, and Conductivity for the Binary Systems of Water + Dual Amino-Functionalized Ionic Liquids

Zanxia Wang,[†,‡] Li Fu,*[,†] Hui Xu,[‡] Ying Shang,[‡] Li Zhang,[‡] and Jianmin Zhang*[,‡]

[†]State Key Laboratory of Solidification Processing, Northwestern Polytechnical University, Xi-an 710072, P. R. China

[‡]Key Laboratory of Green Process and Engineering, Beijing Key Laboratory of Ionic Liquids Clean Process, Institute of Process Engineering, Chinese Academy of Sciences, Beijing, 100190, P. R. China

ABSTRACT: The density, viscosity, and conductivity were investigated for binary mixtures of water and three ionic liquids (ILs), respectively: (3-aminopropyl) tributylphosphonium L-α-aminopropionic acid salt ([aP_{4443}][Ala]), (3-aminopropyl) tributylphosphonium L-α-aminoisovaleric acid salt ([aP_{4443}][Val]), and (3-aminopropyl) tributylphosphonium L-α-amino-4-methylvaleric acid salt ([aP_{4443}][Leu]). The mole fractions of water increased from 0.00 to 0.75, and the temperature varied from (298.15 to 343.15) K. It was found that the viscosity decreased while conductivity increased with the increase of temperature and water content. As the alkyl side-chains of the amino acid anions which might play a role of steric hindrance were lengthened, the density (ρ), viscosity (η), and conductivity (σ) follow the order of $\rho_{[aP4443][Ala]} > \rho_{[aP4443][Val]} > \rho_{[aP4443][Leu]}$, $\eta_{[aP4443][Ala]} < \eta_{[aP4443][Val]} < \eta_{[aP4443][Leu]}$, and $\sigma_{[aP4443][Ala]} > \sigma_{[aP4443][Val]} > \sigma_{[aP4443][Leu]}$, respectively. The temperature-dependent density is fit for the quadratic equation. The temperature dependence of viscosity and conductivity can be described by the Vogel−Tammann−Fulcher (VTF) equation.

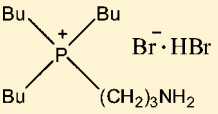

1. INTRODUCTION

The emission of carbon dioxide from burning fossil fuels is the main cause of the greenhouse effect which threatens the environment and sustainable development. Worldwide scientists focused their attention on attempting to find efficient methods to capture CO_2 produced by the industrial process.[1] So far, the most effectively utilized reagent to separate CO_2 is an aqueous solution of alcohol amine to form carbamates.[2−4] However, these alkaline solutions have some serious drawbacks, including volatility, corrosion, and high energy consumption.[5,6] Therefore, it is important to seek sorbent materials with favorable characteristics such as high capacity, stability, and energy saving for CO_2 absorption.[7]

In recent years, functional ionic liquids (ILs) offered alternative candidates to develop new CO_2 capture systems. The first synthesized amino-functionalized IL which is based on the imidazolium structure was utilized for the chemisorption of CO_2 with a saturated mole ratio of 1:0.5.[8] A series of tetrabutylphosphonium ([$P(C_4)_4$][AA])[9] and dual amino-functionalized phosphonium ([aP_{4443}][AA])[10] based amino acid ILs and their absorption behaviors of CO_2 were carried out subsequently. Unfortunately, the ILs became viscous after the uptake of carbon dioxide which is disadvantageous for further saturation from a kinetic viewpoint. To enhance the diffusion rate of carbon dioxide, ILs were coated on a porous silica gel with improved repeatability and stability. The nonvolatile macromolecular solvent PEG 200[11] was also added into ILs as a liquid support to increase the kinetics of the absorption and desorption of CO_2. It was reported that small quantities of water could dramatically decrease the viscosity of the ILs.[12] Thus, a mixture of water and ILs might result in an attractively low viscosity. But, up to now, the properties of the binary systems of ILs plus water have not been reported systematically.

In this work, we reported accurate data for the density, viscosity, and conductivity of binary mixtures containing water and three different ILs, respectively: (3-aminopropyl) tributylphosphonium L-α-aminopropionic acid salt ([aP_{4443}][Ala]), (3-aminopropyl) tributylphosphonium L-α-aminoisovaleric acid salt ([aP_{4443}][Val]), and (3-aminopropyl) tributylphosphonium L-α-amino-4-methylvaleric acid salt ([aP_{4443}][Leu]) from (298.15 to 343.15) K with the mole fraction of water varied from 0.00 to 0.75. Futhermore, the carbon dioxide absorption by the water + [aP_{4443}][Ala] binary system was investigated.

2. EXPERIMENTAL SECTION

Chemicals. Tri-*n*-butylphosphine, 3-bromopropylamine hydrobromide, acetonitrile, ethanol, *n*-hexane, and anion exchange resin 711(Cl) were of analytical grade and produced by Beijing Chemical Reagent Plant. Three natural amino acids, namely, glycine (Gly), L-leucine (Leu), and L-valine (Val), were of biotechnology grade and purchased from Beijing Solarbio Science & Technology Co., Ltd., China. Carbon dioxide (purity of 99.9 %) was purchased from Beijing Hua Yuan Gas Chemical Industry Co., Ltd. The procedure for the synthesis of [aP_{4443}][AA] was similar to the reaction route reported[10] (see Figure 1). The structures of the ILs studied in this work are shown in Figure 2.

The final products obtained were dried in a vacuum oven containing P_2O_5 at 353.15 K for 48 h to remove the residual water prior to use. The water content in the final ILs was below 50 ppm which was analyzed by Karl Fischer titration (Metrohm 756 KF coulometer). The structures of ILs were proved by ^{1}H NMR (Bruker MSL 600) and in good agreement with the literature.[10] The purity of these three ILs in mole fraction is not

Received: September 14, 2011
Accepted: February 29, 2012
Published: March 13, 2012

 © 2012 American Chemical Society

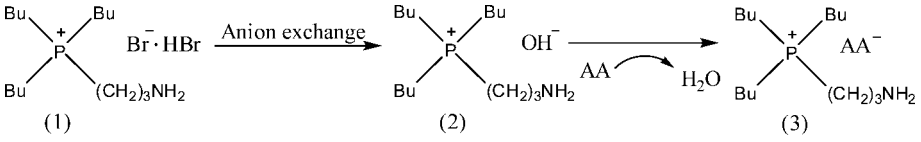

Figure 1. Preparation of $[aP_{4443}][AA]$: 1, $[aP_{4443}][Br]\cdot HBr$; 2, $[aP_{4443}][OH]$; 3, $[aP_{4443}][AA]$.

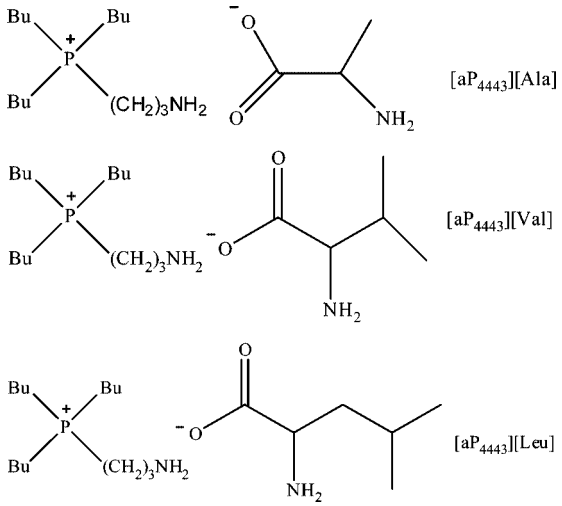

Figure 2. Structures of $[aP_{4443}][AA]$.

less than 99 %. The binary systems of water and ILs were prepared gravimetrically using a precise analytical balance (Mettler Toledo AE 160) within an accuracy of 0.0001 g. In this process, a magnetic stirrer was used to mix the binary systems. All of the samples were prepared soon before density, conductivity, and viscosity measurements.

Density Measurements. The density was measured at atmospheric pressure using a U-type densitometer (Anton Paar DMA 5000, Anton Paar Co., Austria). This instrument was fully automated; therefore, the temperature was controlled with an automatic thermostat with an accuracy of ± 0.001 K. The precision of the density apparatus was within $1\cdot10^{-5}$ g·cm^{-3}, which was calibrated with dry air and ultrapure water.

Viscosity Measurements. The dynamic viscosity was investigated in a Paar AMVn (Anton Paar Co., Austria) viscosity meter, in which the falling time of a ball through liquids was measured according to Höppler's falling ball principle. This instrument was controlled by a computer, and the temperature was controlled by a built-in precise Peltier thermostat. The uncertainty of temperature was ± 0.01 K. At that time, the absolute room pressure was approximately 101 kPa. The repeatability of the viscosity measurement was about ± 2 %.

Conductivity Measurements. The electric conductivity was determined by a conductivity meter (DDJS-308A, Shanghai Leici Company) with a DJS-1C electrode. During this experiment, caution was taken to prevent evaporation, and the electrode and the solution were sealed in typical glassware, which was immersed into a constant temperature oil bath with an accuracy of ± 0.05 K. The uncertainty of the conductivity data was ± 1 %.

Absorption of CO_2. About 1.0 g sample was placed in a typical glass container and agitated with a magnetic bar at room temperature, then CO_2 was fed into the container and bubbled at the flow rate of 60 mL·min^{-1} at atmospheric pressure. The amount of CO_2 absorbed was determined at regular intervals by the analytical balance.

3. RESULTS AND DISCUSSION

The experimental density, dynamic viscosity, and conductivity of the water + $[aP_{4443}][Ala]$, water + $[aP_{4443}][Val]$, and water + $[aP_{4443}][Leu]$ binary systems over the temperature from (298.15 to 343.15) K and different mole fractions of water are listed in Tables 1 to 3.

Density. From Tables 1 to 3, it can be seen that the density of the pure $[aP_{4443}][AA]$ ILs varies from (0.97186 to 0.98675) g·cm^{-3} at 298.15 K. Compared with the corresponding pure pyridinium, ammonium, or imidazolium ILs, they are somewhat lower, which is mainly due to that the larger $[aP_{4443}]$ cation results in weakening ion−ion interactions and blocking ion

Table 1. Density, Viscosity, and Conductivity for H_2O (1) + $[aP_{4443}][Ala]$ (2)

	T/K					
χ_1	298.15	303.15	313.15	323.15	333.15	343.15
			ρ/g·cm^{-3}			
0.00	0.98675	0.98372	0.97765	0.97162	0.96571	0.95977
0.25	0.98847	0.98539	0.97918	0.97304	0.96697	0.96089
0.50	0.99140	0.98827	0.98201	0.97581	0.96957	0.96330
0.75	0.99998	0.99676	0.99022	0.98357	0.97689	0.97015
			η/mPa·s			
0.00	804.88	561.40	291.07	164.61	106.70	65.96
0.25	597.85	417.93	222.26	127.07	78.92	53.07
0.50	429.73	304.20	163.31	95.01	59.30	39.29
0.75	208.66	150.37	83.45	50.38	32.59	22.27
			σ/μS·cm^{-1}			
0.00	140.54	209.48	320.17	464.38	648.92	884.08
0.25	244.02	320.27	487.22	727.42	1009.56	1420.91
0.50	336.97	438.62	702.72	1054.78	1465.65	1926.06
0.75	646.65	859.12	1341.31	1953.28	2647.87	3335.13

dx.doi.org/10.1021/je2007549 | J. Chem. Eng. Data 2012, 57, 1057−1063

Table 2. Density, Viscosity, and Conductivity for H_2O (1) + $[aP_{4443}][Val]$ (2)

	T/K					
χ_1	298.15	303.15	313.15	323.15	333.15	343.15
			ρ/g·cm^{-3}			
0.00	0.98072	0.97768	0.97157	0.96545	0.95950	0.95354
0.25	0.98282	0.97976	0.97359	0.96739	0.96139	0.95537
0.50	0.98718	0.98404	0.97771	0.97155	0.96534	0.95905
0.75	0.99589	0.99265	0.98616	0.97959	0.97296	0.96629
			η/mPa·s			
0.00	1015.49	695.04	350.86	192.24	114.05	72.45
0.25	734.22	508.12	259.52	145.61	87.86	56.87
0.50	505.63	335.23	184.22	102.76	65.77	43.81
0.75	237.96	168.93	92.15	56.03	36.96	24.58
			σ/μS·cm^{-1}			
0.00	81.52	109.69	187.92	294.17	446.83	649.85
0.25	115.58	157.99	252.89	392.39	562.95	858.39
0.50	168.36	237.13	400.58	634.87	930.12	1318.09
0.75	414.03	546.91	853.15	1277.62	1832.06	2579.12

Table 3. Density, Viscosity, and Conductivity for H_2O (1) + $[aP_{4443}][Leu]$ (2)

	T/K					
χ_1	298.15	303.15	313.15	323.15	333.15	343.15
			ρ/g·cm^{-3}			
0.00	0.97186	0.96880	0.96268	0.95654	0.95054	0.94458
0.25	0.97397	0.97091	0.96475	0.95856	0.95254	0.94654
0.50	0.97804	0.97490	0.96861	0.96252	0.95626	0.94999
0.75	0.98711	0.98389	0.97744	0.97088	0.96427	0.95761
			η/mPa·s			
0.00	1227.86	855.26	417.90	224.29	130.46	81.01
0.25	920.24	629.98	308.75	169.80	101.73	65.08
0.5	599.52	407.91	209.07	116.62	72.42	47.47
0.75	244.81	174.05	94.21	55.71	35.35	23.97
			σ/μS·cm^{-1}			
0.00	79.97	108.38	184.80	290.68	413.53	604.67
0.25	113.85	154.09	254.27	379.37	542.22	760.79
0.50	172.94	231.71	361.93	515.26	735.34	1035.21
0.75	395.26	515.17	794.73	1161.62	1610.12	2138.18

packing.[13−15] The difference in the anions with the same $[aP_{4443}]$ cation in the ILs leads to different densities. Figure 3 reveals that the density of pure ILs followed the order of $[aP_{4443}][Ala] > [aP_{4443}][Val] > [aP_{4443}][Leu]$, which is consistent with prior reports that the density decreases with alkyl side-chains length of the amino acids anions.[9,16]

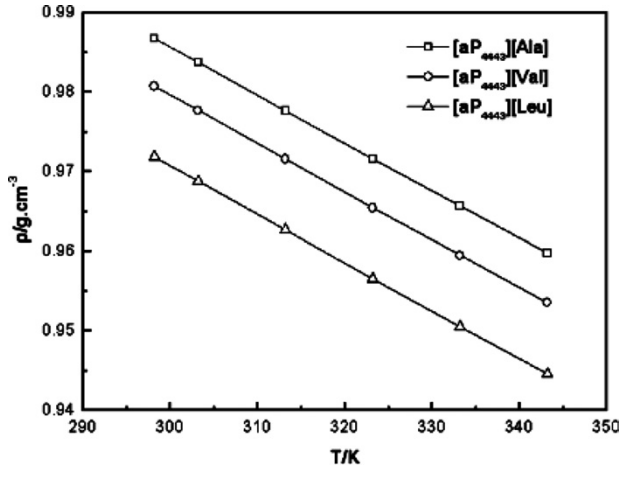

Figure 3. Density variation of the pure $[aP_{4443}][AA]$ ILs with temperature.

Table 4. Parameters of Equation 1 and Standard Deviation Density Correlation of H_2O (1) + $[aP_{4443}][AA]$ (2)

		A_0	A_1	A_2	standard deviations
IL	χ_1	g·cm^{-3}	10^{-4} g·cm^{-3}	10^{-7} g·cm^{-3}	10^{-5} g·cm^{-3}
$[aP_{4443}][Ala]$	0.00	1.1913	−7.6148	2.5257	2.13
	0.25	1.1927	−7.4743	2.0972	1.79
	0.50	1.1754	−6.1601	−0.1244	2.08
	0.75	1.1619	−4.3831	−3.5096	1.89
$[aP_{4443}][Val]$	0.00	1.1895	−7.8334	2.8002	3.13
	0.25	1.1936	−7.9055	2.7977	3.99
	0.50	1.1800	−6.6630	0.6566	4.98
	0.75	1.1621	−4.7009	−2.9269	7.70
$[aP_{4443}][Leu]$	0.00	1.1812	−7.8458	2.7727	2.72
	0.25	1.1842	−7.8701	2.7569	3.59
	0.50	1.1621	−6.1333	−0.1396	5.92
	0.75	1.1485	−4.4172	−3.3359	1.17

dx.doi.org/10.1021/je2007549 | J. Chem. Eng. Data 2012, 57, 1057−1063

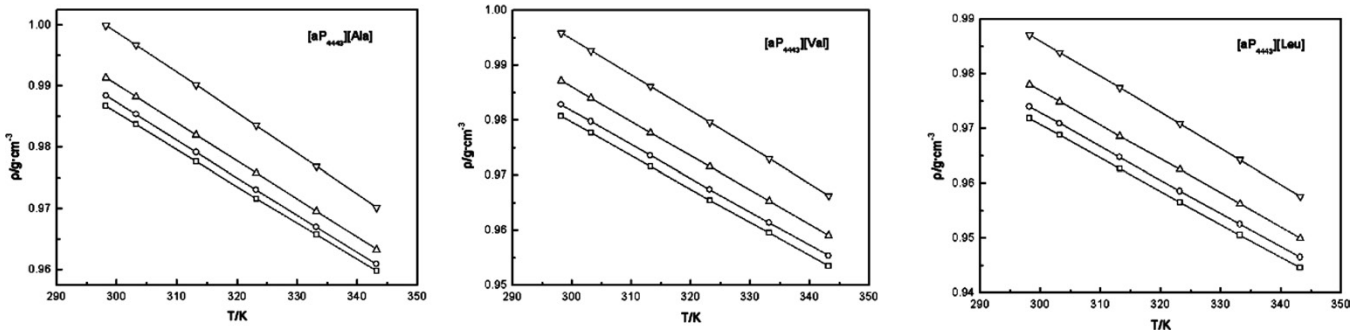

Figure 4. Density for the binary systems as a function of temperature over different mole fractions of water: □, 0.00; ○, 0.25; △, 0.50; ▽, 0.75.

Figure 4 shows that the experimental density for the binary systems, as a function of temperature at different compositions. The density decreases with higher temperature, while increases with the increase in water content. The temperature-dependent density (ρ) can be fitted by the quadratic equation as follows:

$$\rho = A_0 + A_1 T + A_2 T^2 \quad (1)$$

where ρ stands for the density, T is the absolute temperature, and A_0, A_1, and A_2 refer to the fit coefficients. The adjustable parameters of eq 1 for the density of $[aP_{4443}][AA]$ and standard deviations are listed in Table 4.

Dynamic Viscosity. The viscosity is strongly dependent on the type of anion and cation. As illustrated in Figure 5, the relationship of the pure ILs is $[aP_{4443}][Ala] < [aP_{4443}][Val] < [aP_{4443}][Leu]$ (804.88 < 1015.49 < 1227.86 mPa·s) at 298.15 K. The viscosity of the $[aP_{4443}][AA]$ ILs is also strongly affected by the alkyl side-chains of $[AA]^-$. The mobility of the ILs decreases with the lengthening of the alkyl side-chains of $[AA]^-$, and this leads to the highest viscosity of $[aP_{4443}][Leu]$ among three ILs investigated. The viscosity values of the three pure $[aP_{4443}][AA]$ ILs are somewhat higher than those reported by Zhang et al.,[10] where the water content was not mentioned. However, the order of the viscosity is the same.

Unlike density, the influence of temperature on viscosity is much more important. The viscosity can drastically decrease with temperature, especially at lower temperatures (Figure 6). Such as, pure $[aP_{4443}][Val]$ has a viscosity of 1015.49 mPa·s at 298.15 K, which decreases to 350.86 mPa·s at 313.15 K and 114.05 mPa·s at 333.15 K, respectively. The temperature

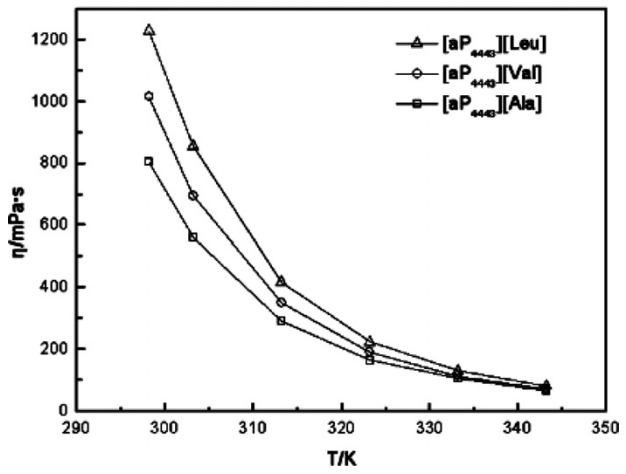

Figure 5. Viscosity variation of the pure $[aP_{4443}][AA]$ ILs with temperature.

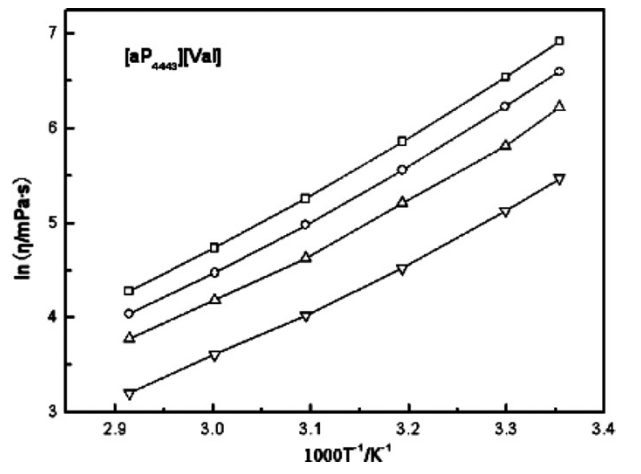

Figure 7. Temperature dependence of viscosity by the VTF equation: χ_1 = □, 0.00; ○, 0.25; △, 0.50; ▽, 0.75.

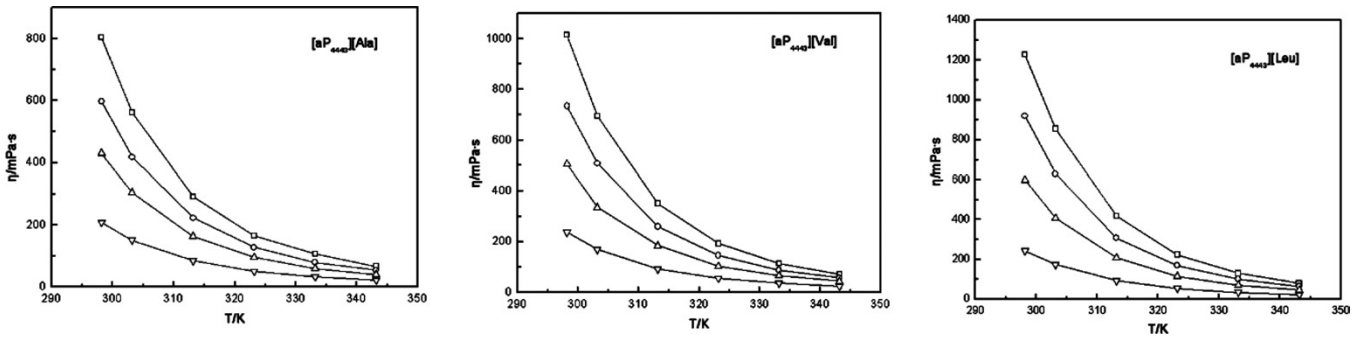

Figure 6. Viscosity for the binary systems as a function of temperature over different mole fractions of water: □, 0.00; ○, 0.25; △, 0.50; ▽, 0.75.

dx.doi.org/10.1021/je2007549 | J. Chem. Eng. Data 2012, 57, 1057–1063

Table 5. VTF Equation Parameters of Viscosity for H_2O (1) + $[aP_{4443}][AA]$ (2)

IL	χ_1	η_0 / mPa·s	B / K	T_0 / K	R^2
$[aP_{4443}][Ala]$	0.00	0.5809	654.7	207.71	0.999
	0.25	0.4795	648.8	207.18	0.999
	0.50	0.3453	668.1	204.54	0.999
	0.75	0.3240	576.1	209.15	0.999
$[aP_{4443}][Val]$	0.00	0.4671	703.7	206.64	1.000
	0.25	0.4063	687.9	206.49	0.999
	0.50	0.6109	545.9	216.85	0.999
	0.75	0.4422	526.1	214.50	0.999
$[aP_{4443}][Leu]$	0.00	0.3044	824.2	199.00	0.999
	0.25	0.4134	696.0	207.94	0.999
	0.50	0.1191	902.9	192.23	0.999
	0.75	0.3071	589.9	209.93	0.999

Table 6. VTF Equation Parameters of Conductivity for H_2O (1) + $[aP_{4443}][AA]$ (2)

IL	χ_1	σ_0 / 10^3 $\mu S \cdot cm^{-1}$	B / K	T_0 / K	R^2
$[aP_{4443}][Ala]$	0.00	40.65	546.2	200.79	0.999
	0.25	54.18	504.4	205.57	0.999
	0.50	55.03	437.9	212.50	0.999
	0.75	39.95	279.3	230.60	0.999
$[aP_{4443}][Val]$	0.00	62.22	648.9	201.38	0.999
	0.25	63.66	604.6	203.86	0.999
	0.50	63.84	501.1	214.35	0.999
	0.75	178.64	623.5	196.45	0.999
$[aP_{4443}][Leu]$	0.00	49.9	632.5	200.36	0.999
	0.25	34.51	517.9	207.96	0.999
	0.50	537.13	1270.6	140.04	0.999
	0.75	72.08	488.4	204.66	0.999

Table 7. Saturated Absorption Capacity of Water + $[aP_{4443}][Ala]$ with CO_2 at Atmospheric Pressure and Room Temperature

χ_1	0.00	0.25	0.50	0.75
M_{CO_2}/M_{IL}	0.46	0.57	0.73	0.40

dependence of the viscosity (η) values for the water + ILs can be described by the Vogel–Tammann–Fulcher (VTF) equation:[17]

$$\eta = \eta_0 \exp\left[\frac{B}{T - T_0}\right] \quad (2)$$

where T is the absolute temperature, η_0 (mPa·s), B (K), and T_0 (K) are adjustable parameters, and T_0 is related to the ideal glass transition temperature. Figure 7 gives an example of temperature dependence of viscosity which is linearized by taking the logarithm of VTF eq 2. Therefore, this equation can be used to predict viscosity values among the temperature range measured. The best-fit parameters for viscosity over the temperature range studied are tabulated in Table 5.

The relationship between viscosity and mole fraction of water at different temperatures is shown in Figure 8. Apparently, the viscosity of the three ILs decreases rapidly with the increasing mole fraction of water, especially at lower temperatures. For example, at 298.15 K, when equal amounts of water were added, the viscosity of pure $[aP_{4443}][Ala]$ (804.88 mPa·s) decreases to 429.73 mPa·s, while it only decreases to 65.96 mPa·s from 39.29 mPa·s at 343.15 K.

Conductivity. It is well-known that the conductivity is related to both the number of charge carrier ions and mobility, which can be expressed by the following equation[18]

$$\sigma = \sum n_i u_i q_i \quad (3)$$

where n_i, q_i, and μ_i are the number of charge carriers, charge, and mobility of pure component i. As illustrated in Figure 9, the conductivity relationship of the pure ILs is $[aP_{4443}][Ala]$ > $[aP_{4443}][Val]$ > $[aP_{4443}][Leu]$ (140.54 > 81.52 > 79.97 $\mu S \cdot cm^{-1}$) at 298.15 K. The main reason is that conductivity is dependent on the mobility of ILs and decreases with viscosity.

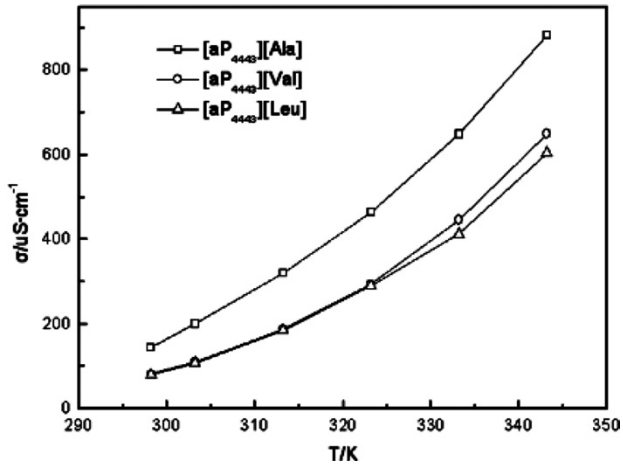

Figure 9. Conductivity variation of the pure $[aP_{4443}][AA]$ ILs with temperature.

The temperature dependence of conductivity of the mixtures is shown in Figure 10. As is observed, the conductivity increases

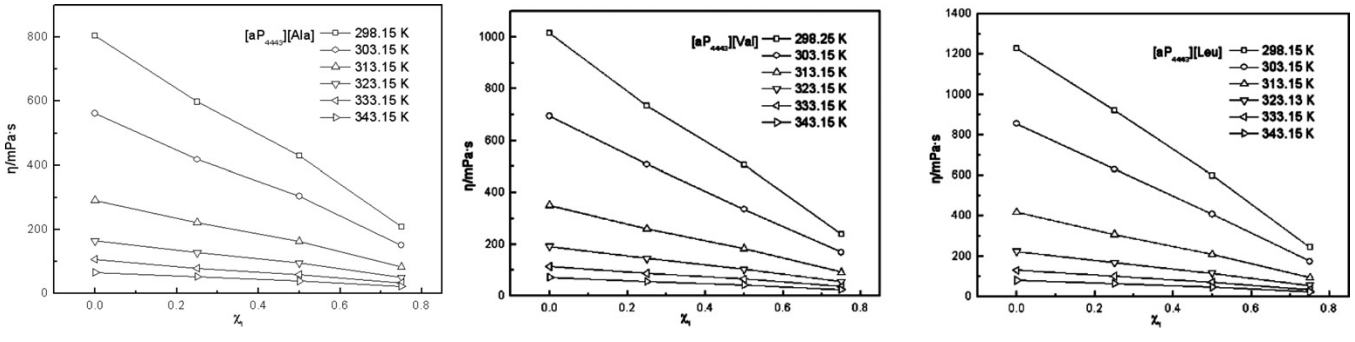

Figure 8. Variation of viscosity vs mole fraction of water for binary systems at different temperatures.

dx.doi.org/10.1021/je2007549 | J. Chem. Eng. Data 2012, 57, 1057–1063

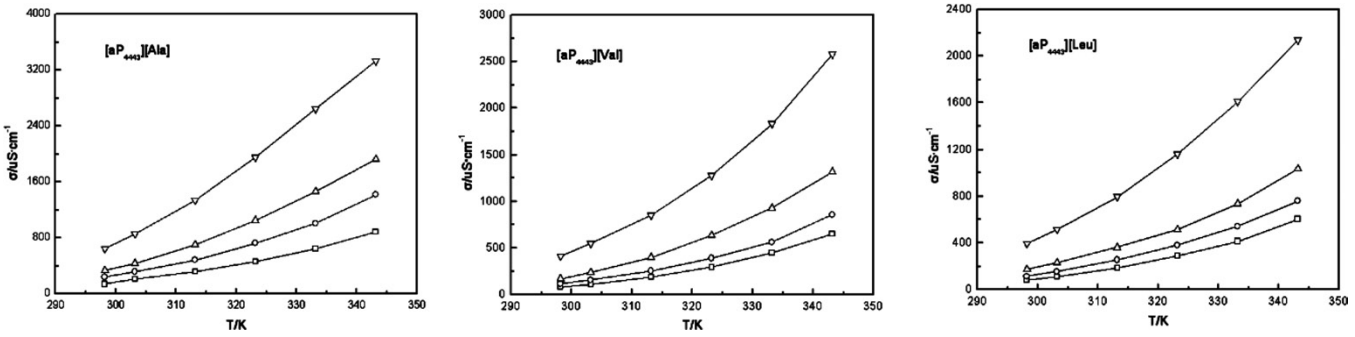

Figure 10. Conductivity for the binary systems as a function of temperature over different mole fractions of water: □, 0.00; ○, 0.25; △, 0.50; ▽, 0.75.

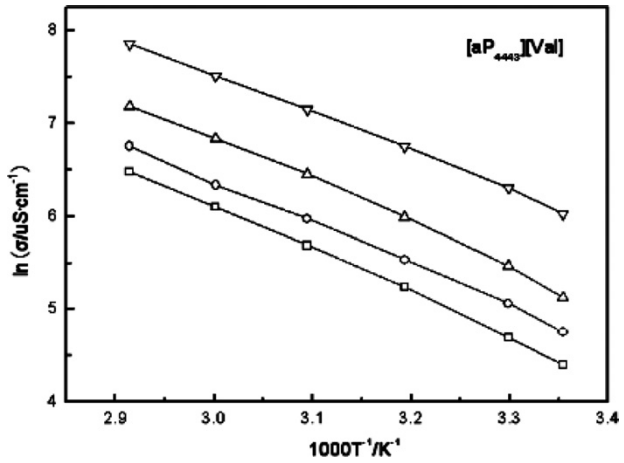

Figure 11. Temperature dependence of conductivity by VTF equation: χ_1 = □, 0.00; ○, 0.25; △, 0.50; ▽, 0.75.

with the increasing of temperature. The VTF equation for conductivity is

$$\sigma = \sigma_0 \exp\left[\frac{-B}{T - T_0}\right] \quad (4)$$

where σ_0, B, and T_0 are constants. In Figure 11, the natural logarithm of σ versus the inverse of absolute temperature for water + $[aP_{4443}][Val]$ binary system, that is, ln σ versus 1000 T^{-1}, is plotted. The best-fit parameters for conductivity are summarized in Table 6.

The conductivity for the water + IL systems versus the mole fraction of water at different temperatures is shown in Figure 12. It increases with the increase in water content, especially at low temperatures. In ILs, a three-dimensional network of anions and cations linked by hydrogen bonds could be formed,[19] and the aggregate structures of the ILs are broken when water was added which would promote the dissociation degree of the ILs.

The VTF equation parameters (T_0) of viscosity and conductivity are summarized in Tables 5 and 6 in which the values of T_0 for the pure ILs agree with the experimental T_g values[10] within experimental error. From the equation parameter (T_0), we also find that T_0 deduced from either viscosity or conductivity is approximately close. So we can predict the glass transition temperature either from the temperature dependence of viscosity or that of conductivity.

In the view that $[aP_{4443}][Ala]$ has the lowest viscosity among those three ILs, the absorption of CO_2 by the water + $[aP_{4443}][Ala]$ binary system was investigated, and the results are summarized in Table 7. From the table we can see that the saturated absorption of CO_2 kept increasing when the mole fraction of water is less than 0.50, while decreasing at 0.75, which means appropriate water could improve the absorption behavior.

4. CONCLUSION

In this work, the density, viscosity, and conductivity of water + $[aP_{4443}][Ala]$, water + $[aP_{4443}][Val]$, and water + $[aP_{4443}][Leu]$ systems were studied under different conditions. In these three binary systems, the [Ala] anion led to the highest density and lowest viscosity. It was also demonstrated that viscosity and conductivity were more sensitive to the changes in water content or temperature than density. The viscosity decreases while conductivity increases with the increase in temperature and water content. The temperature dependence of density is consistent with quadratic equation and is proved to be linear during the temperature range investigated. The temperature-dependent viscosity and conductivity can be described and predicted by the VTF equation.

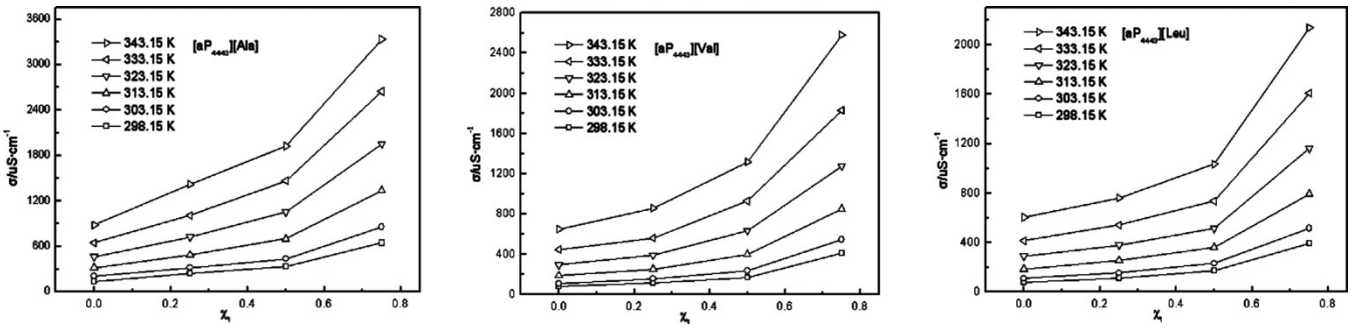

Figure 12. Variation of conductivity vs mole fraction of water for binary systems at different temperatures.

dx.doi.org/10.1021/je2007549 | J. Chem. Eng. Data 2012, 57, 1057–1063

AUTHOR INFORMATION

Corresponding Author

*Tel./fax: +86-029-88491699. E-mail address: fuli@nwpu.edu.cn (L.F.). Tel./fax: +86-010-62550850. E-mail address: jmzhang@home.ipe.ac.cn (J.Z.).

Funding

This work is supported by National Basic Research Program of China (973 Program) (No. 2009CB219901), General Program of National Natural Science Foundation of China (No. 50974113), Open Research Fund of State Key Laboratory of Multiphase Complex Systems (Institute of Process Engineering, Chinese Academy of Sciences), and the Research Fund of the State Key Laboratory of Solidification Processing (NWPU) of China (Grant No. 78-QP-2011).

Notes

The authors declare no competing financial interest.

REFERENCES

(1) George, M.; Weiss, R. G. Chemically reversible organogels: aliphatic amines as "latent" gelators with carbon dioxide. *J. Am. Chem. Soc.* **2001**, *123*, 10393−10394.

(2) Park, S. H.; Lee, K. B.; Hyun, J. C.; Kim, S. H. Correlation and prediction of the solubility of carbon dioxide in aqueous alkanolamine and mixed alkanolamine solutions. *Ind. Eng. Chem. Res.* **2002**, *41*, 1658−1665.

(3) Gabrielsen, J.; Michelsen, M. L.; Stenby, E. H.; Kontogeorgis, G. M. A model for estimating CO_2 solubility in aqueous alkanolamines. *Ind. Eng. Chem. Res.* **2005**, *44*, 3348−3354.

(4) Da Silva, E. F.; Svendsen, H. F. Ab initio study of the reaction of carbamate formation from CO_2 and alkanolamines. *Ind. Eng. Chem. Res.* **2004**, *43*, 3413−3418.

(5) Alejandre, J.; Rivera, J. L.; Mora, M. A. Force field of monoethanolamine. *J. Phys. Chem. B* **2000**, *104*, 1332−1337.

(6) Gutowski, K. E.; Maginn, E. J. Amine-functionalized task-specific ionic liquids: a mechanistic explanation for the dramatic increase in viscosity upon complexation with CO_2 from molecular simulation. *J. Am. Chem. Soc.* **2008**, *130*, 14690−14704.

(7) Yu, G. R.; Zhang, S. J.; Yao, X. Q.; Zhang, J. M.; Dong, K. Design of task-specific ionic liquids for capturing CO_2: a molecular orbital study. *Ind. Eng. Chem. Res.* **2006**, *45*, 2875−2880.

(8) Bates, E. D.; Mayton, R. D.; Davis, J. H. CO_2 capture by a task-specific ionic liquid. *J. Am. Chem. Soc.* **2002**, *124*, 926−927.

(9) Zhang, J. M.; Zhang, S. J.; Dong, K.; Zhang, Y. Q.; Shen, Y. Q.; Lv, X. M. Supported absorption of CO_2 by tetrabutylphosphonium amino acid ionic liquids. *Chem.—Eur. J.* **2006**, *12*, 4021−4026.

(10) Zhang, Y. Q.; Zhang, S. J.; Lv, X. M.; Zhou, Q.; Fan, W.; Zhang, X. P. Dual amino-functionalised phosphonium ionic liquids for CO_2 capture. *Chem.—Eur. J.* **2009**, *15*, 3003−3011.

(11) Li, X. Y.; Hou, M. Q.; Zhang, Z. F. Absorption of CO_2 by ionic liquid/polyethylene glycol mixture and the thermodynamic parameters. *Green Chem.* **2008**, *10*, 879−884.

(12) Seddon, K. R.; Stark, A.; Torres, M. J. Influence of chloride, water, and organic solvents on the physical properties of ionic liquids. *Pure Appl. Chem.* **2000**, *72*, 2275−2287.

(13) Huddleston, J. G.; Visser, A. E.; Reichert, W. M.; Willauer, H. D.; Broker, G. A.; Rogers, R. D. Characterization and comparison of hydrophilic and hydrophobic room temperature ionic liquids incorporating the imidazolium cation. *Green Chem.* **2001**, *3*, 156−164.

(14) Nishida, T.; Tashiro, Y.; Yamamoto, M. Physical and electrochemical properties of 1-alkyl-3-methylimidazolium tetrafluoroborate for electrolyte. *J. Fluorine Chem.* **2003**, *120*, 135−141.

(15) Bonhote, P.; Dias, A. P.; Papageorgiou, N.; Kalyanasundaram, K.; Gratzel, M. Hydrophobic, highly conductive ambient-temperature molten salts. *Inorg. Chem.* **1996**, *35*, 1168−1178.

(16) Gardas, R. L.; Ge, R.; Goodrich, P.; Hardacre, C.; Hussain, A.; Rooney, D. W. Thermophysical properties of amino acid-based ionic liquids. *J. Chem. Eng. Data* **2010**, *55*, 1505−1515.

(17) Fang, S. H.; Yang, L.; Wang, J. X.; Li, M. T.; Tachibana, K.; Kamijima, K. Ionic liquids based on functionalized guanidinium cations and TFSI anion as potential electrolytes. *Electrochim. Acta* **2009**, *54*, 4269−4273.

(18) Every, H.; Bishop, A. G.; Forsyth, M.; MacFarlane, D. R. Ion diffusion in molten salt mixtures. *Electrochim. Acta* **2000**, *45*, 1279−1284.

(19) Li, W. J.; Zhang, Z. F.; Han., B. X.; Hu, S. Q.; Xie, Y.; Yang, G. Y. Effect of water and organic solvents on the ionic dissociation of ionic liquids. *J. Phys. Chem. B* **2007**, *111*, 6452−6456.